Millimeter-wave, Terahertz, and Infrared Devices

Academic and Research Staff

Professor Qing Hu

Visiting Scientists and Research Affiliates

Dr. Gert de Lange

Graduate Students

Hans Callebaut, Erik Duerr, Kostas Konistis, Ben Williams, Noah Zamdmer

1 Introduction

Millimeter-wave and THz frequencies (f > 100 GHz) remain one of the most underdeveloped frequency ranges, even though the potential applications in remote sensing, spectroscopy, plasma diagnostics, and communications are obviously great. This is because the millimeter wave and far-infrared frequency range falls between two other frequency ranges in which conventional semiconductor devices are usually operated. One is the microwave frequency range, and the other is the near-infrared and optical frequency range. Semiconductor devices which utilize the classical diffusive transport of electrons, such as diodes and transistors, have a high frequency limit. This limit is set by the transient time and parasitic RC time constants. Currently, electron mobility and the smallest feature size which can be fabricated by lithography limit the frequency range to below several hundred GHz. Semiconductor devices based on quantum mechanical interband transitions, however, are limited to frequencies higher than those corresponding to the semiconductor energy gap, which is higher than 10 THz for most bulk semiconductors. Therefore, a large gap exists from 100 GHz to 10 THz in which very few devices are available.

Semiconductor quantum-effect devices (which can be loosely termed "artificial atoms"), including both vertically grown quantum-well structures and laterally confined mesoscopic devices, are human-made quantum mechanical systems in which the energy levels can be chosen by changing the sizes of the devices. Typically, the frequency corresponding to the intersubband transitions is in the millimeter-wave range (ΔE ~ 1-4 meV) for the lateral quantum-effective devices, and THz to infrared for the vertical quantum wells. It is therefore appealing to develop ultrahigh-frequency devices, such as radiation detectors and mixers, and THz and infrared lasers utilizing the intersubband transitions in these devices.

In addition to new physical concepts, novel technologies must also be developed to meet the challenges at these high frequencies. Conventional mechanically machined horn antennas integrated with waveguide cavities have been the work horse at microwave and millimeter-wave frequencies since they were first implemented more than fifty years ago during World War II. Very high antenna gain and essentially perfect antenna efficiency can be achieved using these structures. However, they are

expensive, bulky, and incompatible with arrays. In order to overcome these problems, new development has been made to use micromachining to fabricate the horn antenna structures. In these structures, the active elements and their planar antennas are fabricated on a free-standing thin (~1 micron) SiN membrane, which is suspended over a silicon pyramidal horn that is formed by anisotropic etching, or micromachining. The side walls of this micromachined structure can then be coated with Au to form a horn antenna. Compared to conventional waveguide horn antennas, this novel micromachined structure has several major advantages. It is easier to fabricate fine three-dimensional structures by using photolithography. Horn antennas with micron precision can be easily defined and inexpensively mass produced. It is made on Si or GaAs wafers and compatible with thin-film technology. Thus, active elements, such as RF and IF amplifiers, mixers and video detectors, local oscillators, and post-detection signal processors, can be integrated monolithically with the antenna structures to form monolithic transmitter/receiver systems. It is light-weight and compact. The most attractive feature of the micromachined structure is that focal-plane arrays can be fabricated easily on a single wafer, as illustrated in Fig. 1(b). Such systems will yield a significantly improved spatial resolution in remote sensing, and a much greater antenna gain when implemented with phased-arrays.

In our group, we are systematically investigating physical and engineering issues that are relevant to devices operating from millimeter-wave to infrared frequencies. Specifically, we are working on micromachined millimeter-wave focal-plane arrays, and development of terahertz and infrared lasers based on intersubband transitions.

2 Micromachined SIS millimeter-wave focal-plane arrays

Sponsors

National Science Foundation

Grant 9423608-AST

National Aeronautics and Space Administration

Grant NAGW-4691

Project Staff

Gert de Lange, Kostas Konistis, and Qing Hu, in collaboration with Dr. Gerry Sollner and Group 86 at MIT Lincoln Laboratory.

SIS (superconductor-insulator-superconductor) heterodyne receivers have been demonstrated to be the most sensitive receivers throughout 30-840 GHz frequency range. The challenge now in the SIS receiver technology is to develop focal-plane arrays to improve the efficiency of data acquisition. In order to achieve these goals, we are currently developing a novel scheme to couple the millimeter-wave and infrared signals to the superconducting devices by using a micromachined horn antenna and a planar

antenna supported by a thin (~1 micron) membrane, as shown in Fig. 1(a). As stated in the introduction, this novel micromachined antenna structure can be produced with a high precision using photolithography, and it can be utilized in focal-plane arrays, as shown in Fig. 1(b).

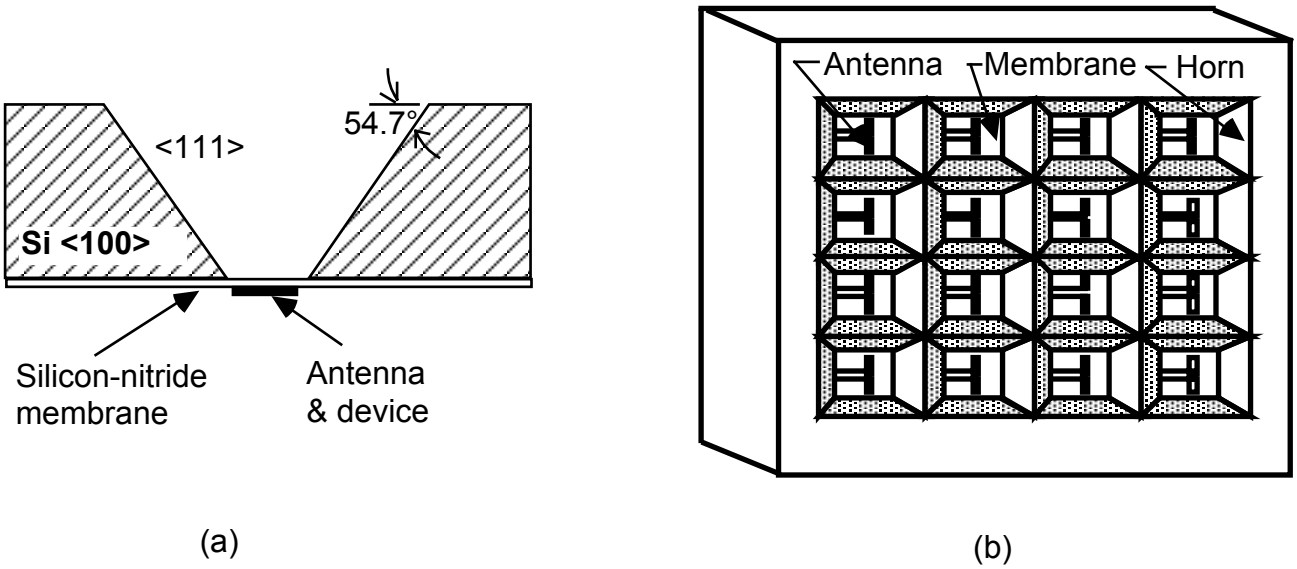

Figure 1. (a) Example of a micromachined horn antenna structure that is made by anisotropically etching a <100> silicon wafer. (b) Schematic of a focal-plane array on a single wafer made using micromachining.

Following our recent success in developing single-element micromachined SIS receivers (see our previous publication in Appl. Phys. Lett. **68**, 1862 (1996)), we have designed and constructed a 3x3 focal-plane array with the center frequency around 200 GHz. The schematic of the structure is shown in Fig. 2, which includes a micromachined and mechanically machined horn array, the device wafer, and the dc and IF connection board. Measurements of the dc I-V characteristics showed good uniformity across the entire array. A heterodyne measurement on the central element yielded the best result. The minimum uncorrected receiver noise temperature is 52 K DSB, measured at a bath temperature of 2.7 K. This noise temperature is comparable to the best results obtained in (tunable) waveguide mixers.

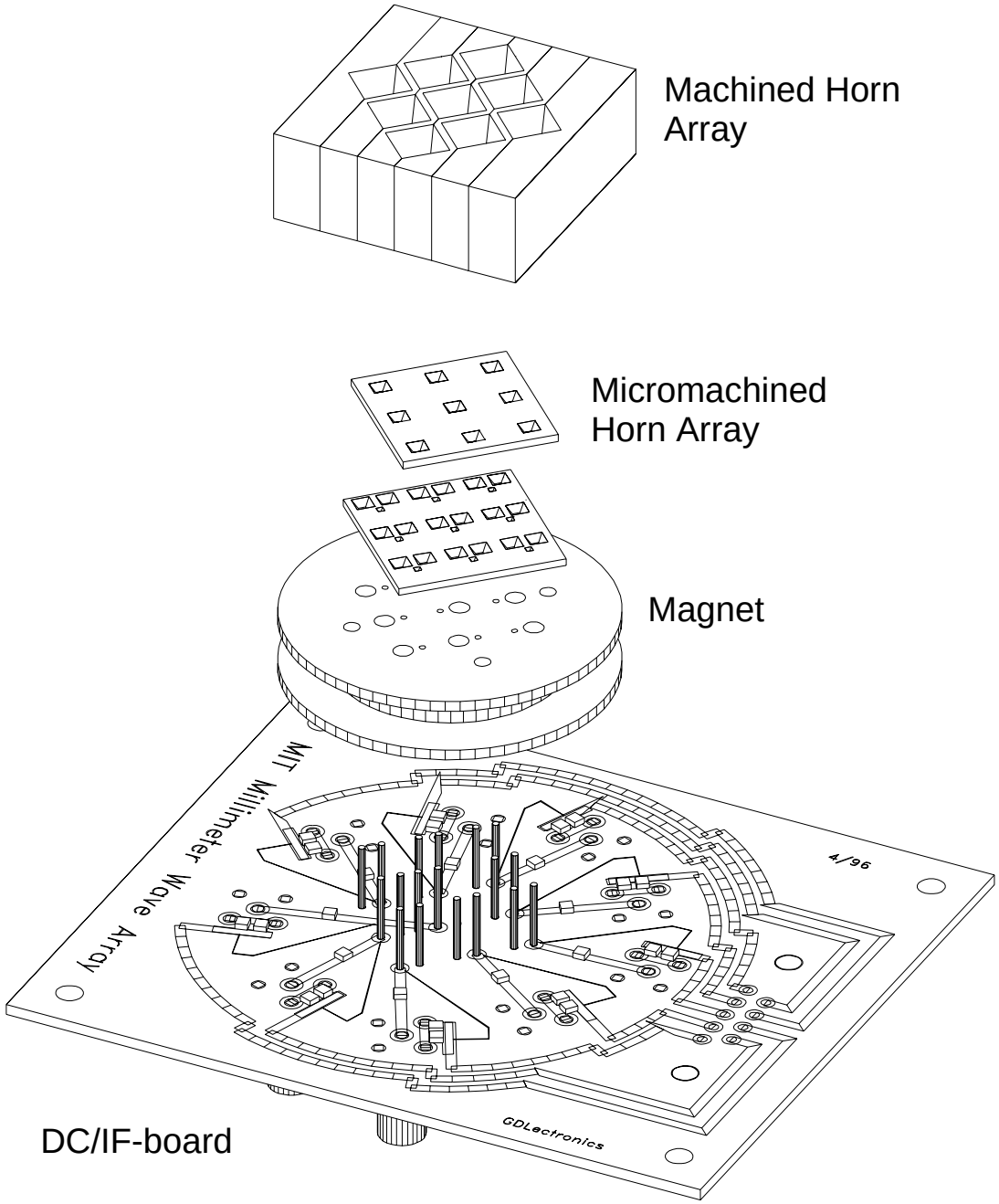

Figure 2. (a) Schematic of an array structure including a micromachined and machined horn array, the device wafer, and the dc and IF connection board. (b) I-V curves of seven SIS junctions in the array.

The measured noise temperatures as functions of the LO frequency for all the 9 elements of another array are shown in Fig. 3. In this array the minimum noise temperature of the central element is 62 K (illustrated in the inset). The measured noise temperature of the different elements is fairly uniform,

with minimum noise temperatures for all the nine elements ranging from 62 to 101 K. The 3-dB noise bandwidth of all the 9 elements has a uniform value of 30 GHz across the array. We attribute the slight difference in the noise temperatures to the effect of the limited size of our dewar window and the thick lens inside the dewar. Measurements of several arrays always showed the lowest noise temperature for the central element. The DSB noise temperatures of the current state-of-the-art waveguide receivers for the 230 GHz astronomy band are in the range of 35-50 K. With a further optimization of the junction device characteristics and a reduction of the junction area, the micromachined SIS mixer arrays could yield comparable noise temperature for each array element. Furthermore, the scalability of the machined and micromachined sections could extend the operating frequencies of the micromachined focal-plane imaging arrays up to 1 THz.

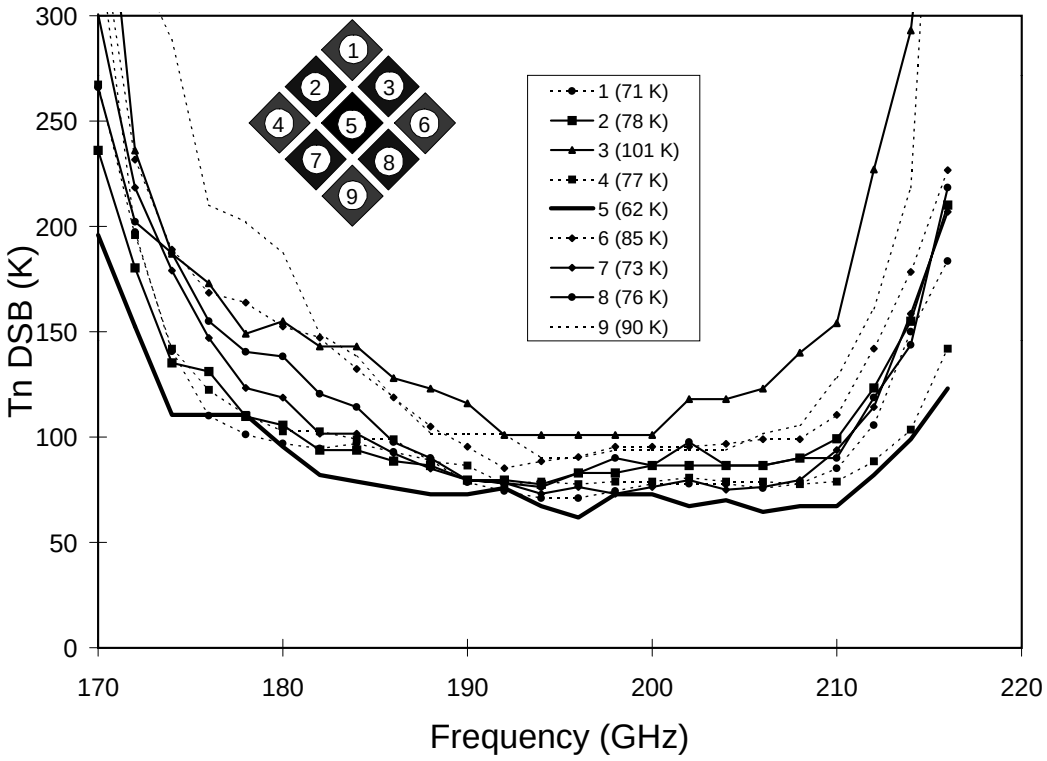

Figure 3. Measured DSB noise temperatures of all the nine elements in the array. The inset shows the minimum noise temperature for each individual element.

3 Terahertz Lasers Based on Intersubband Transitions

Sponsors

National Science Foundation

Grant ECS-9810845

U.S. Army Research Office

Grant DAAD19-99-1-0130

Project Staff

Ben Williams, Hans Callebaut, and Qing Hu, in collaboration with Professor Mike Melloch at Purdue University

Semiconductor quantum wells are human-made quantum mechanical systems in which the energy levels can be designed and engineered to be of any value. Consequently, unipolar lasers based on intersubband transitions (electrons that make lasing transitions between subband levels within the conduction band) were proposed for long-wavelength sources as early as the 1970s. However, because of the great challenge in epitaxial material growth and the unfavorable fast nonradiative relaxation rate, unipolar intersubband-transition lasers (also called quantum-cascade lasers) at near-infrared (4-5 micron) and mid-infrared (8-11 micron) wavelengths were developed only recently at Bell Laboratories. This achievement is remarkable, but the technique used in the original quantum-cascade lasers will not be directly applicable for the longer-wavelength THz range because of two major obstacles. First, the energy levels corresponding to THz frequencies (1 THz = 4 meV) are quite narrow, so the requirements for the design and fabrication of suitable quantum wells are demanding. Because of the narrow separation between subband levels, heating and hot-electron tunneling will have a much greater effect. Also, the small energy scales of THz photons make the detection and analysis of spontaneous emission (a crucial step toward developing lasers) quite difficult. Second and perhaps the most important, mode confinement, which is essential for any laser oscillation, is difficult at longer wavelengths. Conventional dielectric-waveguide confinement is not applicable because the evanescent field penetration, which is proportional to the wavelength and is on the order of several tens of microns, is much greater than the active gain medium of several microns. We are currently developing intersubband-transition lasers based on our recent success in generating and detecting THz emission signals and on a novel mode confinement method using metallic waveguide structures.

Our MQW structure for THz emission is shown in Fig. 4, in which the conduction band profile and the square of the wave functions were calculated self-consistently from Schrödinger and Poisson equations. The device is formed by a triple-well structure using GaAs/$Al_{0.3}Ga_{0.7}As$ materials, as shown in the dashed box. This structure is essentially a three-level system (marked as E_3, E_2, and E_1 in Fig. 4), which is required for any lasers. Because there is no recombination involved in unipolar intersubband lasers, electrons can be “reused” many times. Consequently, many identical triple-well modules can be cascade-connected, and the emission power and the mode confinement factor can be increased substantially. Due to translational symmetry, design analysis needs to focus only on one module, provided

there are no global space charges and high-field domains. The collector barrier (the one marked as B_1) is center δ-doped at approximately $6\times10^{10}/cm^2$ in order to provide dynamic charges to assure a global charge neutrality. The radiative transition takes place between E_3 and E_2, with an energy separation of $\Delta E_{32} \approx 11$ meV (corresponding to 2.7 THz). Under the designed bias of 51 mV per module, the ground state E_1' of a previous module is aligned with E_3. Thus, the upper subband E_3 can be selectively populated through resonant tunneling. The energy separation between E_2 and E_1 was designed to be 40 meV under the bias, which is slightly greater than the LO-phonon energy $\acute{O}\omega_{LO}$ in GaAs. Once energetically allowed, the very fast LO-phonon scattering will rapidly depopulate the E_2 level and establish a population inversion between E_3 and E_2.

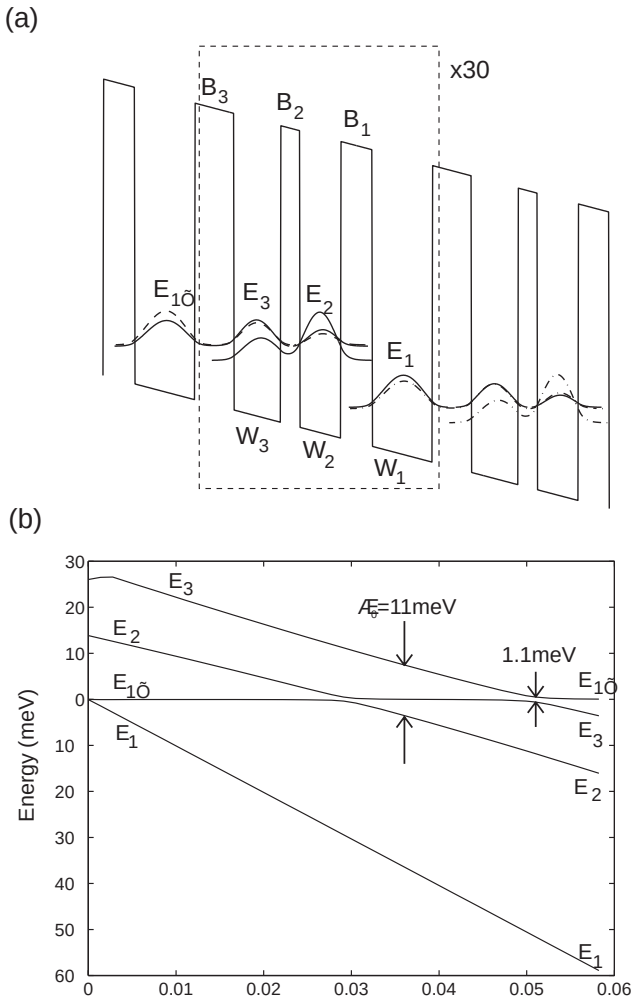

Figure 4. Schematic of a three-level system based on a triple quantum-well structure. The radiation transition takes place between E_3 and E_2, and the fast LO-phonon emission keeps the level E_2 empty. The conduction-band profile and the square of the electron wavefunctions were calculated numerically from Schrödinger and Poisson equations.

In order to measure the intersubband THz emission and resolve its spectra, we constructed a set-up that included an external Fourier transform infrared spectrometer (FTIR) with a composite Si bolometer as its detector. The system's schematic is shown in Fig. 6. We have improved this system and perfected our measurement techniques so that THz emission measurements can be routinely performed on our emitters with output power levels of 1-10 pW.

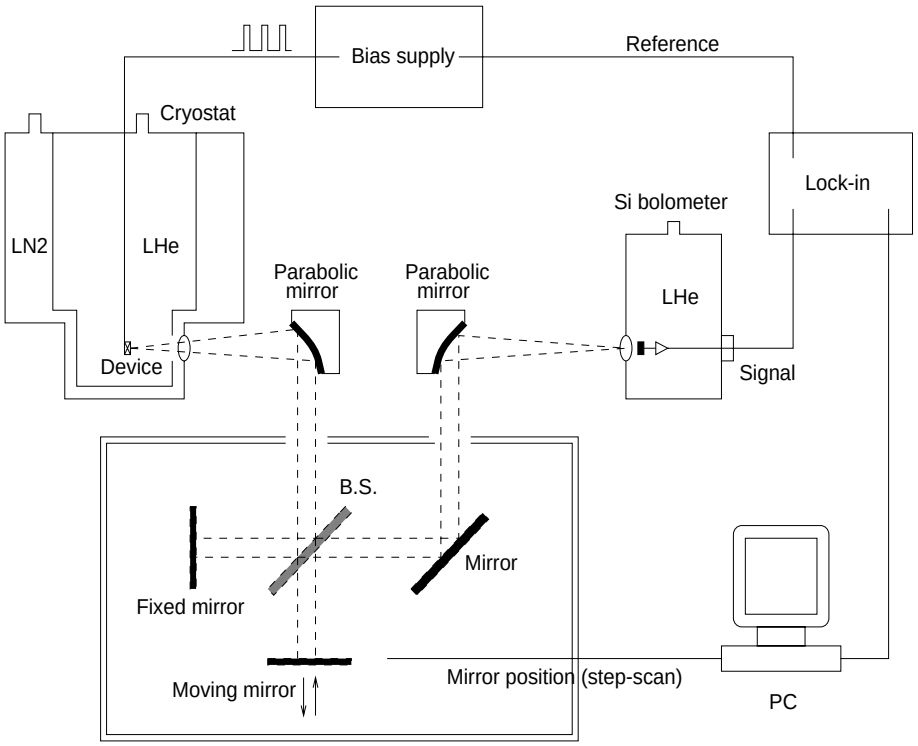

Figure 5. Far-infrared measurement set-up that uses an external Fourier transform spectrometer to spectrally resolve the emitted THz signals.

The MQW structures were grown in the molecular-beam epitaxy (MBE) machine in the group of our collaborator Professor M. R. Melloch at Purdue University. Our optical spectra reveal a clear peak due to the $E_3 \rightarrow E_2$ intersubband emission. A representative spectrum taken at 5 K is shown in Fig. 6(a), which was taken at a bias of 1.6 V (close to the designed value of 1.53 V). The measured peak frequency of 2.57 THz (corresponding to 10.6 meV) is close to the designed value of 11 meV. The full width half maximum (FWHM) of the emission peak is as narrow as 0.47 THz (1.93 meV). Spectra were also taken with the cold stage cooled with liquid nitrogen to 80 K. A measured spectrum is shown in Fig. 6(b). The

main peak is essentially the same as the one measured at 5 K, with only a slightly broader linewidth of 0.52~THz (2.14 meV). The secondary broad feature is blackbody radiation due to device heating. The linewidth measured at 80~K is expected to be similar to that at 5~K, since nonparabolicity is negligible for THz intersubband emitters. Nevertheless, our experimental verification is encouraging for the development of intersubband THz sources at elevated temperatures.

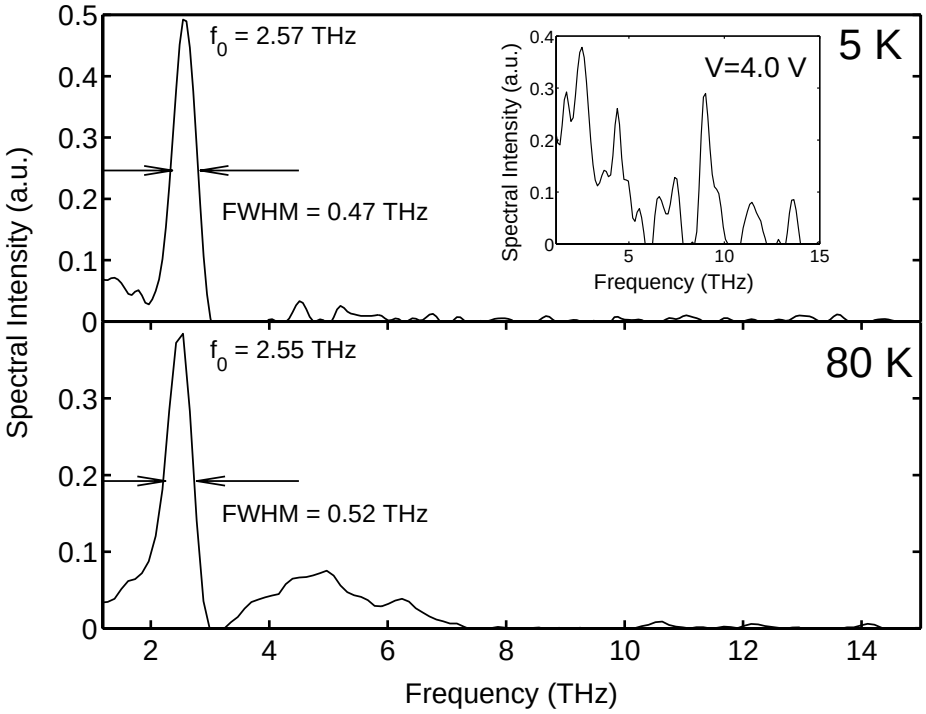

Figure 6. Spectrally resolved THz intersubband emission taken at (a) 5~K and (b) 80~K under a bias of 1.6~V. The inset shows the spectrum under a 4.0~V bias.

4 An on-chip frequency-domain submillimeter-wave transceiver

Sponsor

NSF/MRSEC

Grant 9400344-DMR

Project Staff

Noah Zamdmer and Q. Hu, in collaboration with Dr. S. Verghese at Lincoln Laboratory

Photoconductive emitters and receivers are attractive as components of sub-millimeter-wave spectroscopy systems because of their tunability, compactness and ability to be monolithically integrated with antennas, transmission lines and microelectronic devices. Such systems can be classified in either of

two ways: as time-domain or frequency-domain systems, or as systems involving free-space or on-chip submillimeter wave propagation. Time-domain systems, which contain a photoconductive pulse emitter and sampler excited by a mode-locked laser, are the most investigated. They have been used for free-space characterization of semiconductor materials, and on-chip characterization of ultrafast devices and circuits with 2.7 ps time resolution. The frequency resolution is the inverse of the time span over which the propagating pulse is sampled. This span is determined by the length of an optical delay line, which usually results in a frequency resolution greater than 1 GHz.

A frequency-domain spectrometer was recently introduced with a frequency resolution of better than 1 MHz, which is adequate for molecular line spectroscopy. Its source is a photomixer, which is a voltage-biased antenna-coupled photoconductor that generates a cw output at the difference frequency of the two tunable diode lasers that illuminate it. A photomixer is tunable from DC to about 5 THz, and its linewidth is determined by the stability of the lasers that drive it. The spectrometer's detector is another antenna-coupled photoconductor illuminated by a delayed portion of the two overlapping laser beams that illuminate the source. The light incident on the detector creates a modulated photocarrier density that performs homodyne detection of the continuous wave from the source.

In this project we developed the first on-chip version of the above frequency-domain spectrometer. Such a spectrometer is attractive because it has the frequency resolution required for low-pressure gas spectroscopy. It is also compact and inexpensive, and it can be part of a microfluidic, "lab on a chip"-type circuit. Furthermore, it has the advantage over a free-space spectrometer that it can be used to test microelectronic devices without the collimation and focusing of submillimeter waves. We demonstrate and model an on-chip frequency-domain transceiver which uses low-temperature-grown (LTG) GaAs photoconductors to emit and detect continuous waves in the frequency range from 20 GHz to 700 GHz propagating in a coplanar waveguide circuit. Our device has a possible frequency resolution (~ MHz) that is about 10^3 times better than similar devices used for time-domain spectroscopy, and is therefore appropriate for high-resolution spectroscopy with an integrated circuit. As the first step in the development of an on-chip frequency-domain spectrometer, here we investigate the performance of an on-chip transceiver containing only uninterrupted coplanar waveguides (CPWs).

Our circuit, shown in Fig. 7(a), is the same as the one on which we performed time-domain experiments. The circuit has a biased pump photoconductor and an unbiased probe photoconductor connected by a main CPW, and other parasitic CPWs which provide DC electrical contact to the photoconductors. As illustrated in Fig. 1(a), we excited propagating electromagnetic waves at the pump by illuminating the pump photoconductor with two overlapping diode laser beams with a difference frequency $f = \omega_2-\omega_1$. We performed homodyne detection of those waves by illuminating the probe with a delayed portion of the same laser beams. We describe the relative delay between the pump and probe beams with the phase Φ. We expect the output DC current I_{o1} to vary sinusoidally with Φ because of the homodyne detection performed at the probe photoconductor. We describe this dependence as $I_{o1}(\Phi) = I_o\cos(\Phi+\delta)$. The argument of cosine contains two terms: the phase Φ, which is due only to the path lengths of the pump and probe beams; and the phase δ, which describes the response of the circuit and any device or

specimen inserted in it. For example, δ may be non-zero because of the dispersion of the CPWs or circuit resonance. Our aim was to measure I_o and δ as functions of f. Together, I_o and δ contain all the information necessary for coherent spectroscopy.

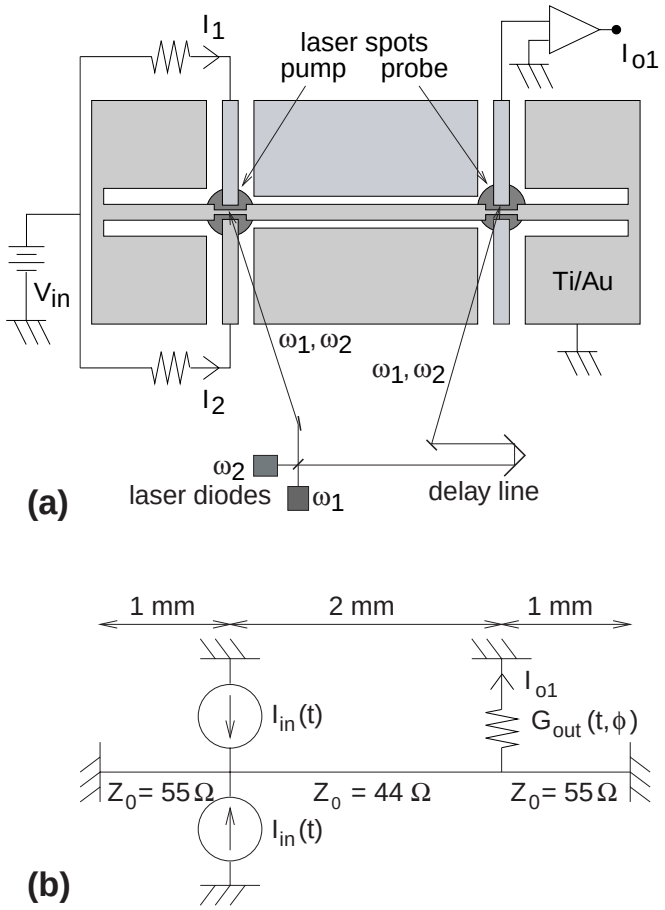

Figure 7. (a): Diagram of the experimental circuit, showing its electrical bias and optical input. (b) Microwave circuit model of the experimental circuit.

We fit the measured spectra to a model based on the circuit shown in Fig. 7(b). The two active regions of the pump photoconductor are modeled as current sources. Similarly, the single utilized active region of the probe photoconductor is modeled as the time-varying conductance. We assume that the two laser diode beams were perfectly overlapped. We also assume that the CPWs have a propagation constant $\Gamma=\alpha(f)+j2\pi f/v_p$, where $\alpha(f)$ is the attenuation constant to be fit to the data, and v_p is the phase velocity of a coplanar transmission line on a semi-infinite GaAs substrate. We use standard microwave circuit analysis to calculate I_{o1}, the Φ-dependent DC current generated at the probe.

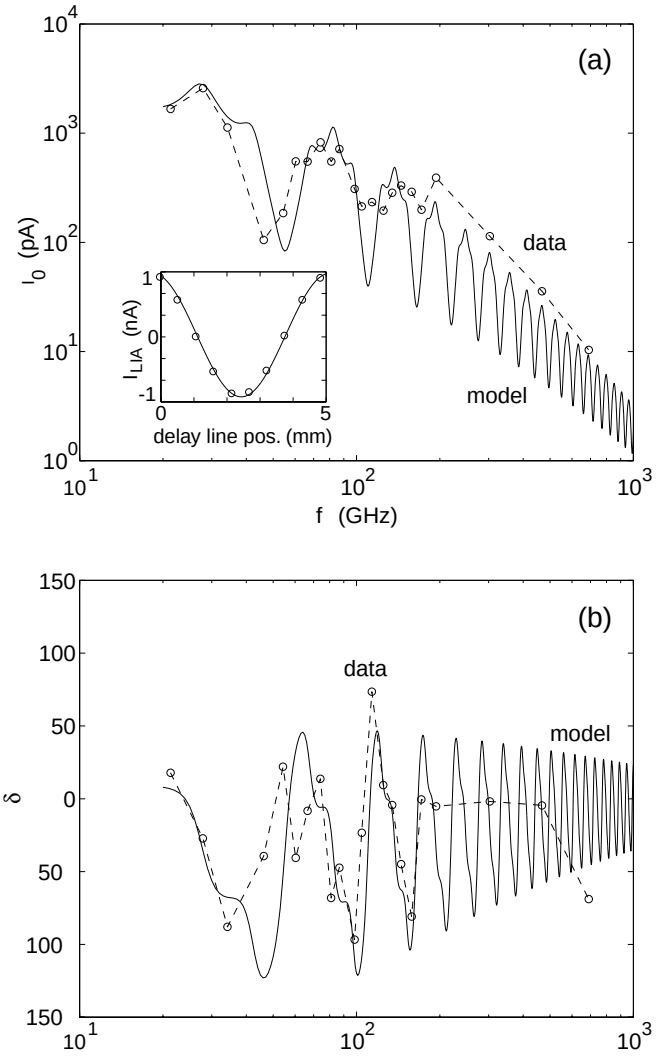

Figure 8. Measured data and model of the amplitude and phase spectra (a) $I_o(f)$ and (b) □(f). Inset: output of lock-in amplifier vs. delay line position at f=27.9 GHz, compared to a best-fit sinusoid.

Our model was fit to the data with reasonable fitting parameters. As shown in Fig. 8, the agreement between the model and the measured results is quite good, validating the microwave-circuit analysis of our on-chip submillimeter-wave transceiver.

5 Publications

1. Zamdmer, Q. Hu, S. Verghese, and A. Förster, “Mode-discriminating photoconductor and coplanar waveguide circuit for picosecond sampling,” Appl. Phys. Lett. **74**, 1039 (1999).

2. Hu, Q. and I. Lyubomirsky, "Response to 'Comment on Energy level schemes for far-infrared quantum-well lasers,'" Appl. Phys. Lett. **74**, 3065 (1999).

3. de Lange, G., K. Konistis, and Q. Hu, "A 3x3 millimeter-wave micromachined imaging array with superconductor-insulator-superconductor mixers," Appl. Phys. Lett. **75**, 868 (1999).

4. Zamdmer, N., Q. Hu, K. A. McIntosh, and S. Verghese, "Increase in response time of low-temperature-grown GaAs photoconductive switches at high voltage bias," Appl. Phys. Lett. **75**, 2313 (1999).

5. Williams, B. S., B. Xu, Q. Hu, and M. R. Melloch, "Narrow-linewidth Terahertz Intersubband Emission from Three-level Systems," Appl. Phys. Lett. **75**, 2927 (1999).

6. Zamdmer, N., Q. Hu, K. A. McIntosh, and S. Verghese, "On-chip frequency-domain submillimeter-wave transceiver," Appl. Phys. Lett. **75**, 3877 (1999).

5.1 Conference presentations

1. Zamdmer, N., Q. Hu, K. A. McIntosh, and S. Verghese, “Theoretical and Experimental Study of a Low-temperature-grown GaAs Photoconductive Switch Under High Voltage Bias,” presented at Ultrafast Electronics and Optoelectronics, Snowmass, Colorado, April 16 (1999).

2. B. S. Williams, B. Xu, Q. Hu, and M. R. Melloch, "Narrow linewidth terahertz intersubband emission from three-level multiple quantum well structures," presented at the 5th International Conference on Intersubband Transitions in Quantum Wells (ITQW'99), Bad Ischl, Austria, September (1999).

3. B. S. Williams, B. Xu, Q. Hu , and M. R. Melloch, "NARROW-LINEWIDTH TERAHERTZ INTERSUBBAND EMISSION FROM THREE LEVEL SYSTEMS." presented at 1999 Material Research Society Fall Meeting, Boston, MA, November 30 (1999). (invited)

Theses

Ph.D. theses

Zamdmer, Noah, thesis title, "The Design and Testing of Integrated Circuits for Submillimeter-wave Spectroscopy," June, 1999.